Journal of the Korean Ceramic Society
Vol. 43, No. 11, pp. 715~723, 2006.

Properties Optimization for Perovskite Oxide Thin Films by Formation of Desired Microstructure

Xingzhao Liu,† Bowan Tao, Chuangui Wu, Wanli Zhang, and Yanrong Li

National Key Laboratory of Electronic Thin Films and Integrated Devices, University of Electronic Science and Technology of China, Chengdu 610054, China
(Received October 19, 2006; Accepted October 30, 2006)

ABSTRACT

Perovskite oxide materials are very important for the electronics industry, because they exhibit promising properties. With an interest in the obvious applications, significant effort has been invested in the growth of highly crystalline epitaxial perovskite oxide thin films in our laboratory. And the desired structure of films was formed to achieve excellent properties. $Y_1Ba_2Cu_3O_{7-x}$ (YBCO) superconducting thin films were simultaneously deposited on both sides of 3 inch wafer by inverted cylindrical sputtering. Values of microwave surface resistance R_S (75 K, 145 GHz, 0 T) smaller than 100 mΩ were reached over the whole area of YBCO thin films by pre-seeded a self-template layer. For implementation of voltage tunable high-quality varactor, A tri-layer structured $SrTiO_3$ (STO) thin films with different tetragonal distortion degree was prepared in order to simultaneously achieve a large relative capacitance change and a small dielectric loss. Highly a-axis textured $Ba_{0.65}Sr_{0.35}TiO_3$ (BST65/35) thin films was grown on $Pt/Ti/SiO_2/Si$ substrate for monolithic bolometers by introducing $Ba_{0.65}Sr_{0.35}RuO_3$ (BSR65/35) thin films as buffer layer. With the buffer layer, the leakage current density of BST65/35 thin films were greatly reduced, and the pyroelectric coefficient of 7.6×10^{-7} C cm^{-2} K^{-1} was achieved at 6 V/μm bias and room temperature.

Key words : Perovskite, YBCO, Superconductor, Thin film, Epitaxial

1. Introduction

Within the class of inorganic materials, oxide are strategically important and are expected to have widespread industrial use, especially the perovskite related oxides with unusual and promising properties. The perovskite oxides containing transition metal cations can yield high conductivity metals, such as $(Ba,Sr)RuO_3$ (BSR), or even superconductors, as with $YBa_2Cu_3O_{7-x}$ (YBCO). Collective phenomenon involving electric dipole interactions in insulators yields ferroelectrics such as $(Ba,Sr)TiO_3$ (BST). With an interest in fundamental properties and the obvious utility in applications, significant effort has been invested in the growth of perovskite oxide thin films. While polycrystalline oxide films may have sufficient properties for some applications, the superior properties of highly crystalline epitaxial films are most attractive both for applications and fundamental studies of material properties.

However, the epitaxial growth of the perovskite oxides is still somewhat of a mystery, possibly because their special nature is not yet fully recognized. First, as the perovskite oxide such as YBCO is only stable in a specific parameter window of substrate temperature (T_s) and oxygen partial pressure (P_{O2}), the deposition conditions are limited within a narrow window. Second, the deposition of multi-metallic species with an accuracy better than 1% is not a simple matter. Moreover, the growth of complex oxide has to be distinguished from that of a simple materials such as metals and elemental semiconductors.

In this paper, the study of perovskite oxide thin film growth in our laboratory are introduced. Results are given to structure and properties of the electronic oxide thin films, with emphasis on structure modification to optimize the properties. By pre-seeding a self-template layer 3 inch double-sided YBCO superconducting thin films with low microwave surface resistance were deposited. In order to simultaneously achieve a large relative capacitance change and a small dielectric loss for voltage tunable varactor, a trilayered $SrTiO_3$ (STO) thin films with different tetragonal distortion degree were grown. Highly a-axis textured $Ba_{0.65}Sr_{0.35}TiO_3$ (BST65/35) thin films with high pyroelectric coefficient were prepared on $Pt/Ti/SiO_2/Si$ substrate for monolithic bolometers by introducing a $Ba_{0.65}Sr_{0.35}RuO_3$ (BSR65/35) buffer layer.

2. Large Size Double-Sided YBCO Thin Films for Microwave Components

High-temperature superconductors have applications in high-performance microwave devices such as resonators, filters and multiplexers for mobile communications.[1] The microwave applications require large area double-sided

†Corresponding author : Xingzhao Liu
E-mail : xzliu@uestc.edu.cn
Tel : +86-28-8320-2140 Fax : +86-28-8320-2569

YBCO thin films with low microwave surface resistance and good homogeneity.

The microwave surface resistance of YBCO thin films is very sensitive to the growth mechanisms, surface morphology and domain structure of the thin films.[2,3] Therefore, the controlled growth of YBCO thin films in an atomic scale becomes an important issue.

The initial growth stage of an epilayer may determine the quality of the ultimate films. In the initial growth stage, the adatoms nucleate on the substrate surface (heteroepitaxy). As the film thickness increases and the coverage is completed, the film continues to grow at the nuclei of the YBCO thin films (homoepitaxy). The surface energy and kinetics of the film growth for the two stages are different. Generally speaking, the surface energy of heteroepitaxy is higher than that of homoepitaxy. Thus a slightly higher T_s is essential for the improvement of the crystal structure of the initial heteroepitaxial layer. Preseeded self-template growth has been carried out by a slight change of the substrate temperature during deposition. For example, the deposition was carried out at 860°C in the initial stage, and the substrate temperature was then decreased to 840°C in the sequential deposition of YBCO thin films. It has been shown that the structure and superconducting properties of YBCO thin films could be significantly enhanced by the preseeded self-template layer.[4,5] Three-inch double-sided YBCO thin films with low microwave surface resistance and excellent lateral homogeneity over the entire area were prepared by a preseeded self-template buffer layer in our laboratory.

A single DC inverted cylindrical sputter gun was arranged to simultaneously deposit YBCO thin films on both sides of the 3-inch $LaAlO_3$ wafer.[6] The superconducting properties of the films were measured by resistance measurements. The critical current density J_c of the films was determined by the standard four-probe method with microbridges of 30×200 μm patterned by photolithography. The microwave surface resistance R_s was measured by the dielectric resonator method operated in the TE_{011} mode at 17 GHz. The power handling capability was determined by R_s(H) measurements at 8.5 GHz and 77 K. The R_s lateral homogeneity over the 3-inch wafer was measured using a Fabry-Perot resonator at 145 GHz and 75 K. R_s, which was determined by using the Fabry-Perot resonator, provides a lateral resolution of about 0.6 mm.

In the XRD patterns of the YBCO thin films prepared with and without the preseeded self-template layer, the θ-2θ scan spectrums showed that all the films are purely c-axis oriented. No grains with other orientation and no impurity phases aredetected in the films. In the φ-scan spectrums from the (308) plane, except the four peaks separated by 90° reflecting the symmetry of YBCO, no other peaks appear. All the films showed that there is only one kind of crystallographic orientation relationship between the substrate and the film in the *a-b* plane. Although there are no differences in the θ-2θ scan spectrums and the φ-scan spectrums of the YBCO thin films prepared with and without the preseeded self-template layer, the Full Width at Half Maximum (FWHM) value of the ω-scan spectrum from the (005) reflection of the film prepared with the preseeded self-template layer is much lower than that of the film prepared without the preseeded self-template layer as shown in Fig. 1. The

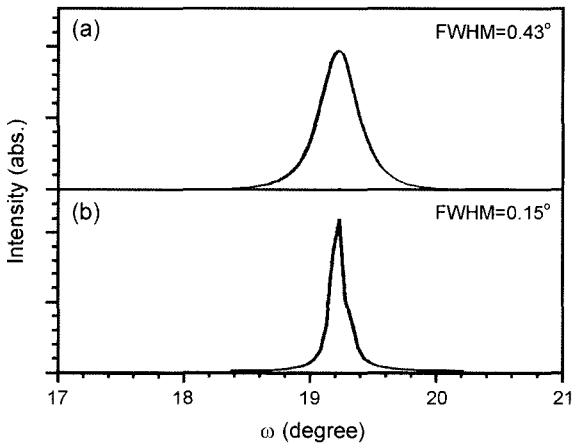

Fig. 1. Rocking curves of YBCO thin films: (a) without the preseeded self-template layer and (b) with the preseeded self-template layer.

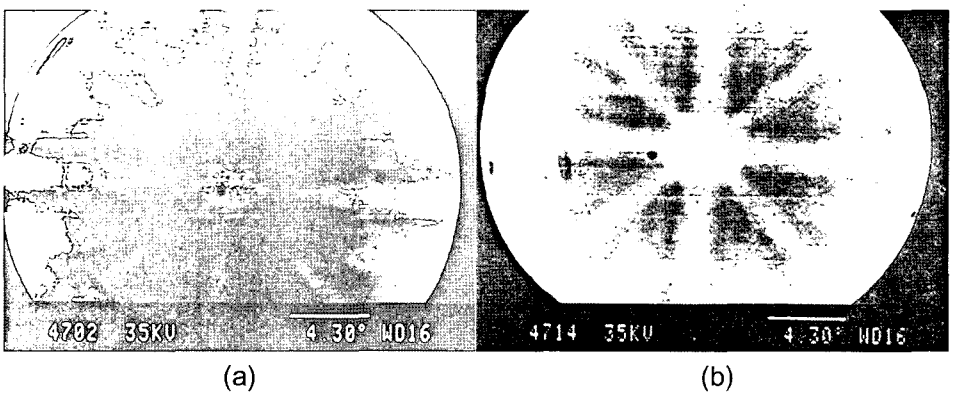

Fig. 2. Electron channeling patterns of YBCO thin films: (a) without the preseeded self-template layer and (b) with the preseeded self-template layer.

FWHM values of the films prepared with and without the preseeded self-template layer are 0.15° and 0.45°, respectively. It showed that the preseeded self-template layer significantly improves the out-of-plane orientation of the YBCO thin films.

The electronic channeling patterns (ECP) of the YBCO thin films are shown in Fig. 2. The ECP of the film prepared with preseeded self-template layer is very sharp, clear and symmetric, indicating a high degree of grain arrangement ordering and a high degree of epitaxy. However the ECP of the film prepared without preseeded self-template layer is poor, indicating the existence of more grains with a misaligned c-axis and larger angle grain boundaries.

The T_c, J_c, and R_s measurements showed excellent agreement between the two sides of the wafers with the the preseeded self- template layer. The T_c value of the films ranges from 89.5 K to 91 K. The typical transition width ranges from 0.5 K to 0.8 K. J_c is in the range of $2\sim3\times10^6$ A/cm^2. The highest magnetic field $\mu_0 H$, which induces the breakdown of microwave properties of the films, is 6 mT as shown in Fig. 3. The R_s (77 K, 8.5 GHz, 0 T) values of YBCO thin films on both sides are 0.2 mΩ. According to the ω^2 law published by Newman and Lyons,[7] the R_s (77 K,10 GHz, 0 T) values are 0.27 mΩ. The consistency between the two sides and the reproducibility are excellent. However, the R_s (77 K, 10 GHz, 0 T) values of the double-sided YBCO thin films without the preseeded self-template layer typically ranged from 0.5 to 0.8 mΩ. The consistency between the two sides and

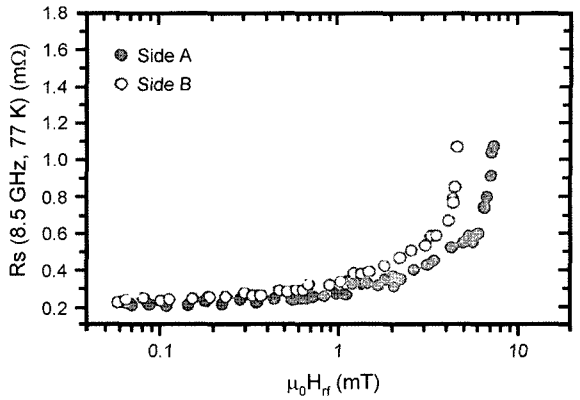

Fig. 3. Power handling capability of the YBCO films grown with preseeded self-template layer.

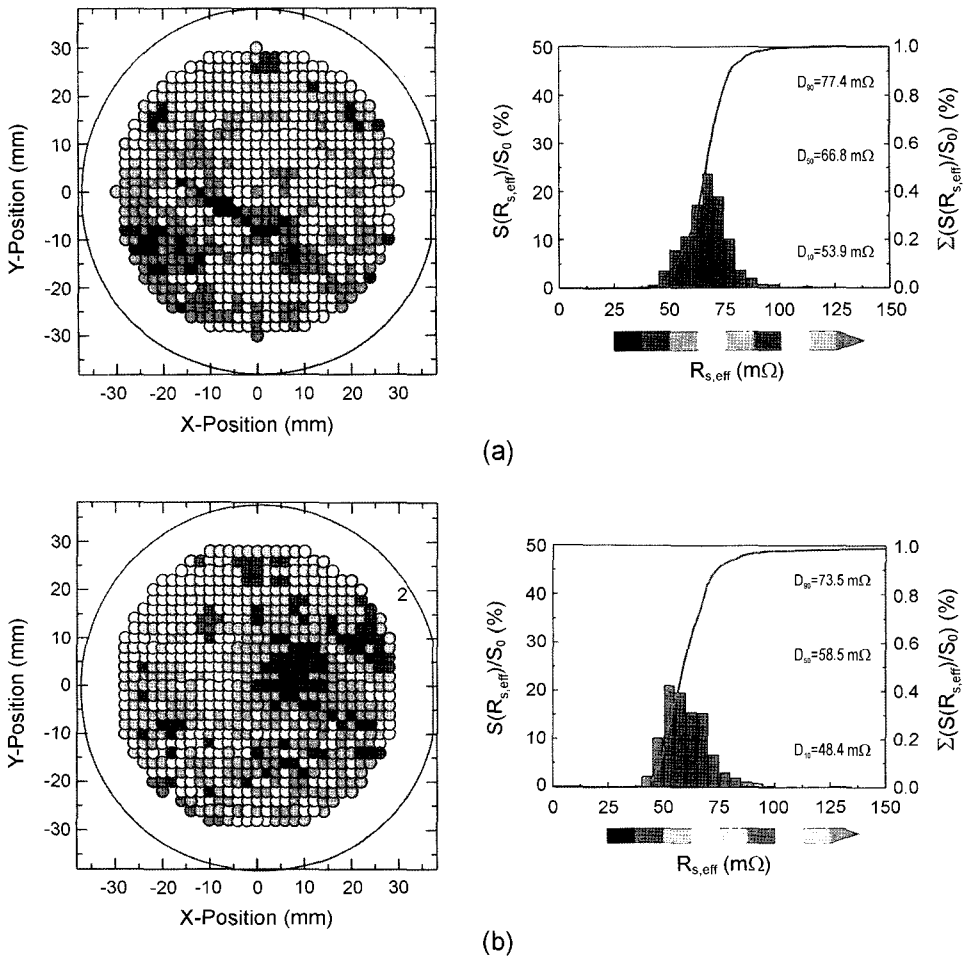

Fig. 4. Lateral homogeneity of the microwave surface resistance R_s maps of the 3-inch double-sided YBCO films grown with preseeded self-template layer.

The microwave resistance lateral homogeneity of the 3-inch double-sided YBCO thin films prepared by using the pre-seeded self-template layer is shown in Fig. 4. The data were collected by measurements at 700 different positions over the entire wafer. The values of microwave surface resistance R_s (75 K, 145 GHz, 0 T) below 100 mΩ were obtained over the entire YBCO thin films on both sides of the 3-inch wafers. The majority of the wafer area on side A has R_s (75 K, 145 GHz, 0 T) values in the range from 54 to 77 mΩ. Nineteen percent of the measuring positions on side A has R_s (75 K, 145 GHz, 0 T) values lower than 77 mΩ. The majority of the wafer area on side B has R_s (75 K, 145 GHz, 0 T) values in the range from 48 to 74 mΩ. Nineteen percent of the measuring positions on side B has R_s (75 K, 145 GHz, 0 T) values lower than 74 mΩ. So the lateral homogeneity on both sides of the wafer and equality between side A and side B are excellent.

3. STO Thin Films for High-Q Voltage Tunable Microwave Components

In general, high temperature superconductors (HTSC) offer a much lower surface resistance than conventional materials at microwave frequency. Ferroelectrics (FE) are a class of nonlinear dielectrics which exhibit an electric field dependent dielectric constant. Due to the similar crystal lattice type of HTSC and perovskite FE, there have been significant interest and effort in combining the low microwave losses in HTSC with the voltage control of FE dielectric constant ε_r, especially $SrTiO_3$ (STO), to implement voltage tunable low loss microwave devices, such as phase shifters, filters, delay lines, and tunable oscillators.[8-11]

A main focus of research for the effective utilization of STO thin films is the development of materials with simultaneously optimized permittivity (absolute magnitude as well as its electric field dependence, etc.) and low dielectric loss (tanδ). However, the tunability and the dielectric loss in thin films have not been comparable to the bulk values. Most STO thin films showed very low dielectric constant, low tunability and large dielectric loss compared with single crystal STO. Many reasons have been suggested for the degradation in the tunable dielectric thin films. A tetragonal distortion (ratio of in-plane and surface normal lattice parameters, D=a/c), a dead layer near the interface, and local polar regions near the charged defects like oxygen vacancy are expected to degrade the dielectric properties of the thin films.[12-14] Among them, the tetragonal distortion in thin films is one of the most critical problems, since the low frequency dielectric properties are closely related to the ionic motions in crystal structures, especially the soft phonon mode.

The oxygen vacancy, the lattice mismatch and the thermal expansion difference between the film and substrate alter the structure of deposited film. Several researchers have reported on the influence of tetragonal distortion caused by the lattice mismatch and the thermal expansion difference on dielectric properties of STO thin films, especially on the dielectric constant.[15,16] Several researchers have investigated the effect of oxygen vacancy on dielectric properties of hetero-epitaxially grown STO thin films.[17,18] It is worthwhile to note that the study of oxygen vacancy is complicated because of the additional effect of film stress due to the film-substrate mismatch and difference in thermal expansion coefficients. There have been no systematic studies on the influence of tetragonal distortion caused by oxygen vacancy on dielectric properties of STO thin films. In our laboratory, STO thin films were homo-epitaxially grown on Nb doped STO (Nb:STO) substrate.[19] No additional stress caused by the lattice constant mismatch and thermal expansion coefficient difference between films and substrate in the STO thin films. Homo-epitaxially grown STO thin film is a good candidate to systematic study the effect of oxygen vacancy on dielectric properties of STO thin films. The study showed that the STO films with low oxygen vacancy concentration demonstrated low zero-bias permittivity, low dielectric tunability, high dielectric dissipation, high breakdown electric field, and the STO films with high concentration of oxygen vacancy exhibited reduced dielectric loss, high dielectric tunability, and low breakdown electric field. In order to make use of the respective advantages of STO thin films with different oxygen vacancy concentration, trilayers were constructed by STO thin films with high oxygen vacancy concentration sandwitched by STO films with few oxygen vacancy in our laboratory.

STO thin films were deposited by Pulsed Laser Deposition (PLD) technique.[19] The tri-layered structure, which was constructed by one thin STO layer with high oxygen vacancy concentration sandwiched by two STO thin films with low oxygen vacancy concentration, was prepared by varying oxygen pressure during deposition. First, a STO thin layer with 100 nm thickness was deposited on a Nb:STO substrate at 10 Pa. Next the oxygen pressure was adjusted to 2 Pa and the second STO thin film with 300 nm thickness was grown. Finally, STO thin film with 100 nm thickness was grown at 10 Pa oxygen pressure as the third layer. The three STO thin layers were sequentially deposited without breaking vacuum.

For low frequency dielectric property measurements, parallel capacitors were made by evaporating Au films onto the STO thin films through shadow masks as the top electrode. The Nb:STO substrate was used as the bottom electrode, and the area of top electrode was 0.2 mm^2. Capacitance and dielectric dissipation of the capacitors were measured using an LCR meter with a signal level of 0.1 Vrms. The leakage current was measured using a digital multimeter. In the measurement of C-V and I-V characteristics, the bias was applied to the Au top electrode, and the Nb:STO substrate was connected to ground terminal. All the measurments were carried out at 77 K.

The crystal structure was characterized by High Resolution X-Ray Diffraction (XRD). The samples used for XRD analysis were deposited on (100) $LaAlO_3$ (LAO) substrate.

Although different substrate impose different film structure due to a differrent lattice mismatch at the film/substrate interface and different thermal expansion coefficients values between the films and substrates,[15,20,21] the effect of substrate on film microstructure focuse on such characters as film texture, dislocation density, and surface morphology etc. When the film thickness is larger than a critical value (only several nanometers for STO film/LAO substrate system), the strain in the films is released by dislocation. The primary effect of misfit strain on the film microstructure presents at the interface. So the effect of oxygen vacancy on the lattice constant is more intrinsic effect when the film is thick enough.[22-25] For the trilayers deposited on Nb doped substrate, because the diffraction peak from the STO thin films with low oxygen vacancy concentration and that from the Nb:STO substrate is too close to separate with each other, the XRD spectrum of the trilayers deposited on LAO substrate was used to characterize the relationship between the lattice constant and oxygen vacancy concentration of STO thin films.

The High Resolution X-rays Diffraction of the trilayer is shown in Fig. 5. With Dual Channel Analyzer (DCA) for Triple Axis X-ray Diffraction (TAXRD) Omega-2.

Theta scan, the diffraction peak of STO trilayer has been split into two peaks. The left one is at −3430 arc second, while the right one is at −3040 arc second. The lattice of an oxygen deficient films expands beyond the size reported for corresponding bulk ceramics. An increasement in the number of oxygen vacancy increase the lattice parameter of the oxide thin films. Kim[26] reported a strong influence of oxygen partial pressure on the lattice parameter of (Ba, Sr)TiO_3 (BST) films. The BST thin films deposited at low oxygen pressure (3~50 mTorr) show large changes along both in-plane (a) and surface normal (c) directions associated with the change of deposition pressure. The TAXRD spectrum as shown in Fig. 5 may be a result of two STO layers with different lattice constant respectively.

The TAXRD Omega scan over STO (002) reflection for both apexes of epilayer peak is shown in Fig. 6. The curve a was measured at fixed Omega-2Theta of −3040 arc second for the left, with FWHM of 1126 arc second, while the curve

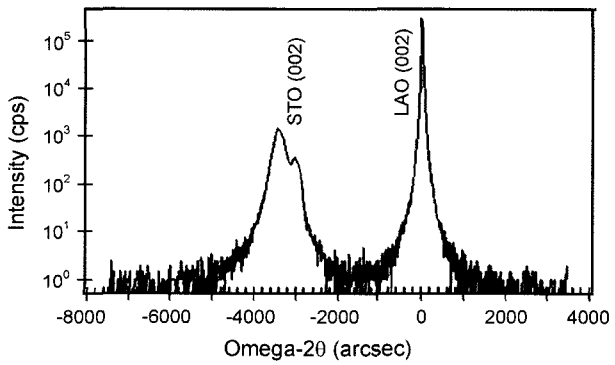

Fig. 5. High resolution X-rays diffraction of the trilayer.

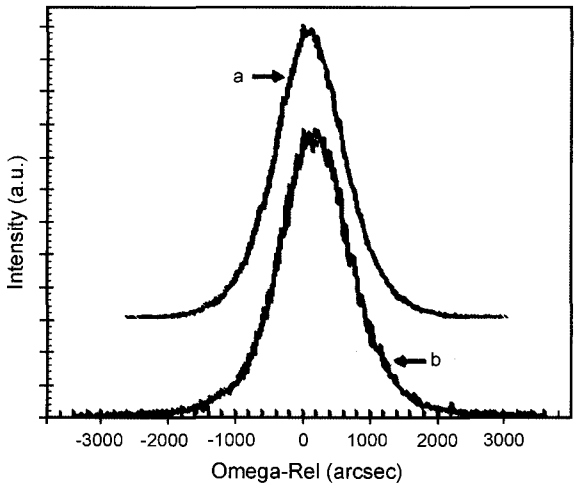

Fig. 6. TAXRD Omega scan over STO(002) reflection for both apexes of epilayer peaks.

b at fixed.

Omega-2Theta of −3430 arc second for the right, with FWHM of 1200 arc second. There is only one symmetric peak in Triple Axis STO (002) Omega scan. The two splits at Omega-2Theta epilayer peak (as shown in Fig. 5) should result from lattice strain, rather than lattice tilt. The FWHM for both apexes of STO epilayer peak is very closed to each other. The crystalline quality is similar for the two STO layers.

The reciprocal space map over STO(103) reflection in reciprocal space units is shown in Fig. 7. The center of the STO (103) reflection located at (1.025, 0, 2.884) and (1.025, 0,

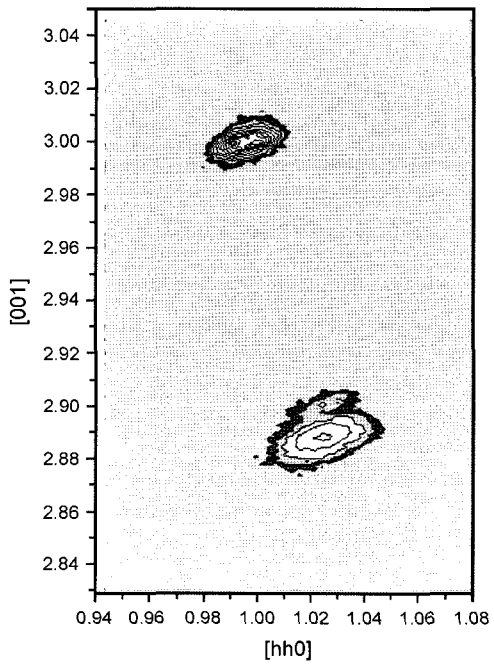

Fig. 7. Reciprocal space map over STO (103) reflection in reciprocal space units.

2.900). This gave the a lattice parameter of STO is 3.918 Å, the c lattice parameters are 3.941 Å and 3.919 Å, corresponding to the left and right epilayer diffraction peak, respectively. The tetragonal distortion degree of the two STO thin layers was 0.9997 and 0.9942 respectively, which shows that the films are fully relaxed. So the trilayer is in fact a multilayer formed by two STO thin layers with different lattice parameters as confirmed by a TAXRD Omega scan and Reciprocal Space Map (RSM).

The leakage current of the tri-layer are shown in Fig. 8. The leakage current density remains at a low level even at the bias voltage of 10 V (The electric field is as high as 200 kV/cm), and thus, the trilayer can withstand large electric field.

The dielectric properties of the trilayer are shown in Fig. 9. Under the electric field of 200 kV/cm, the dielectric constant tunability was 60%. The maximum dielectric loss tangent was 0.75%.

In the trilayer, the middle layer with high oxygen vacancy concentration act as active layer for large tunability. In the meanwhile, the upper and bottom layer with low concentration of oxygen vacancy act as barrier to the de-trapping current of the trapped electrons in the middle layer under high electric field. Thus, the trilayer can not only withstand large electric field, but also large tunability and low dielectric dissipation was achieved.

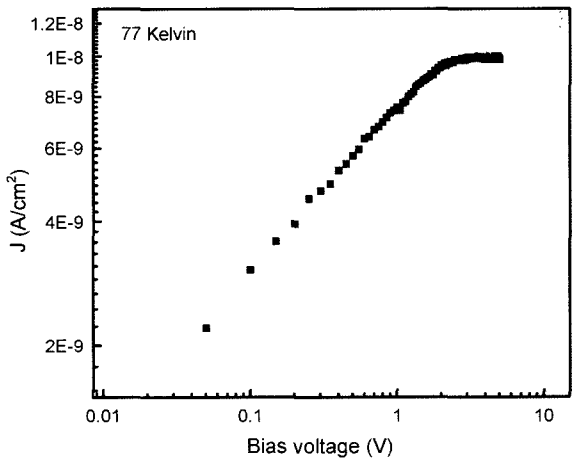

Fig. 8. Leakage current of the trilayer.

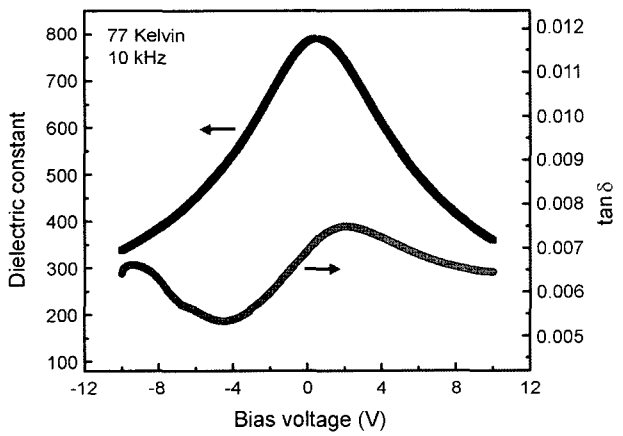

Fig. 9. Dielectric properties of the trilayer.

4. BST Thin Films for Monolithic Bolometers

The ferroelectric bolometers currently in volume production are fabricated through two separate processed wafers, the ceramic array and the silicon readout IC (Si-ROIC), which are then sliced into chips and bonded together as hybrid component. However, poor thermal isolation and thermal crosstalk between pixels in these devices limited their further performances improvement.[27] The monolithic thin film based bolometers, which integrate ferroelectric thin films, such as barium strontium titanate (BST), on micro bridge with existing on-chip Si-ROIC, have the potential for very high thermal isolation, very low thermal mass and negligible thermal crosstalk between pixels.[28,29] It is expected to improve performances of the bolometers', and even to push the Noise-Equivalent-Temperature-Difference (NETD) to approach the theoretical limit of a few mK with smaller pixel. However, the deposition process for ferroelectric thin film needs high temperature which is not compatible with Si-ROIC process. It has hindered the further development of monolithic ferroelectric thin film bolometers. A "composite" device structure,[30] which separates the high temperature fabrication processes from the constraints of the Si-ROIC, was proposed to obtain a good process compatibility of ferroelectric thin film deposition with good performances. However, ferroelectric thin film bolometers still have not achieved a good performance as expected, since ferroelectric thin films have not achieved high pyroelectric coefficient as that of corresponding ferroelectric ceramics.

Usually, some metals like platinum (Pt) with a high work function are employed as an electrode for the BST thin films because they can lead to a low leakage current density by building up a high Schottky barrier at BST/metal interfaces. However, some problems still exist, and it hinders Pt usage as a bottom electrode for BST thin films in practical applications, such as the formation of hillocks at high temperature[31] and amiability in oxygen diffusion.[32] In addition, BST thin films directly deposited on Pt electrode are polycrystalline which exhibit bad properties compared with preferred orientated films.[33]

In our laboratory, $Ba_{0.65}Sr_{0.35}TiO_3$ (BST65/35) thin films with high pyroelectric coefficient were prepared by RF inverted cylindrical sputtering onto $Pt/Ti/SiO_2/Si$ substrate by introducing a thin $Ba_{0.65}Sr_{0.35}RuO_3$ (BSR65/35) buffer layer.[34] A 10 nm amorphous BSR thin film was deposited onto the $Pt/Ti/SiO_2/Si$ substrate first. Then the amorphous BSR layer were in-situ annealed at 700°C for 30 min in vacuum. The thin BSR layer act as a buffer layer for BST thin film deposition.

Capacitance-frequency measurements was performed by

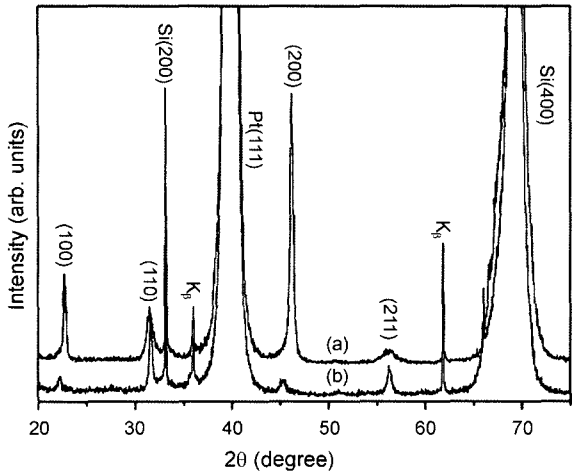

Fig. 10. XRD patterns of BST thin films: (a) with BSR buffer layer and (b) without BSR buffer layer.

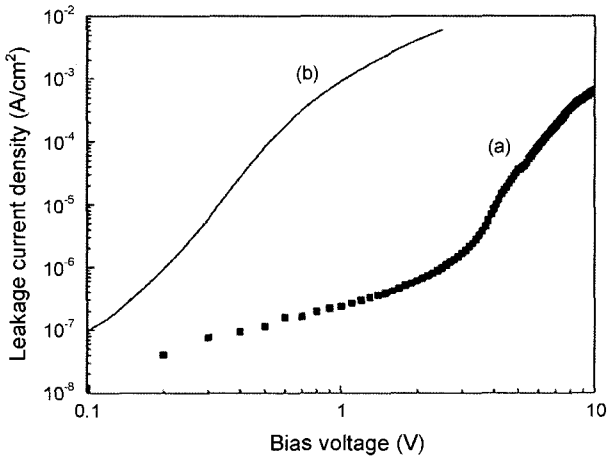

Fig. 11. J-V characteristics of BST thin films: (a) with BSR buffer layer and (b) without BSR buffer layer.

using HP4284A impedance analyzer with an oscillation voltage of 0.1 V from 20 Hz to 1 MHz. The current-voltage characteristic was measured by a HP4155B semiconductor parameter analyzer. The pyroelectric coefficient ρ of the BST thin films was measured by a dynamic technique proposed by Chynoweth.[35]

The XRD patterns of 250 nm BST thin films with and without BSR seeding-layer are shown in Fig. 10. The peaks were consistent with that of the perovskite structure, which indicate a polycrystalline structure. In the case of inserting BSR seeding-layer, the (100) and (200) peaks of BST thin films were significantly enhanced, indicating highly a-axis textured. Since the BSR seeding-layer was only 10 nm thick, distinct X-ray diffraction peaks for this seeding-layer have not been observed. The preferential a-axis orientation parameter were 26.9% and 83.1% for BST thin films without and with BSR seeding-layer, respectively. It indicates that the BSR seeding-layer strongly influence the textured degree of BST thin film. The enhanced preferential a-axis textured degree should be attributed to the structure similarity and very small lattice mismatch between BSR65/35 and BST65/35.

Because leakage current causes the device power loss and the input noise, the leakage current density decrease is a crucial issue and an important technical challenge for ferroelectric bolometers. Fig. 11 shows the leakage current density of BST films with and without BSR buffer layer. It is clear that the leakage current density of BST thin films on BSR seeding-layer was greatly reduced. So the reduction of leakage current density is possibly due to the BSR seeding-layer acting as a good template for BST thin film, which can block grain boundaries in BST thin film.

Fig. 12 shows the voltage response dependence of BST thin films on temperature variation. The bias voltage is 1.5 V. The temperature variation was sinusoidal wave modulated from 294 K to 302 K with frequency of 1/60 Hz. It is clear that the out-put voltage was modulated by the temperature variation. So the voltage response was resulted from the pyroelectric property of the BST thin films, instead of trapped charge releasing. The pyroelectric coefficient obtained from the derivative of the V_{out}-T curve was 7.57×10^{-7} C cm^2 K^1. It is higher than that of BST bulk ceramics (1×10^7 C cm^2 K^1 at 40 kV/cm).[20] Highly a-axis-oriented $Pb(Nb_{0.02}Zr_{0.2}Ti_{0.8})O_3$ thin films was reported to have higher pyroelectric coefficient than that of polycrystalline films.[33] The high pyroelectric coefficient of the BST thin films with BSR seeding-layer should be attributed to the enhanced preferential a-axis texture degree.

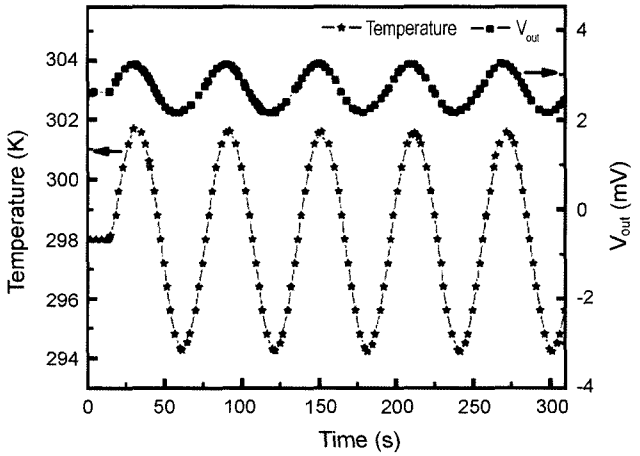

Fig. 12. Pyroelectric response of BST thin films with BSR seeding-layer.

5. Summary

By using a preseeded self-template layer, the crystal structure of YBCO thin films was significantly improved. Three-inch double-sided YBCO thin films with higher degree of epitaxy and good lateral homogeneity were reproducibly prepared. By varying oxygen pressure during depo-

sition, a relaxed STO tri-layer with different oxygen vacancy concentrations was formed. A significantly improved optimization of high tunability and low loss was achieved. By inserting a thin BSR seeding-layer as a good template for BST thin film deposition, BST thin films with highly a-axis textured degree and pyroelectric coefficient as high as 7.57×10^{-7} C cm^2 K^1 was achieved.

REFERENCES

1. A. I. Braginski, "Superconducting Electronics Coming to Market," *IEEE Trans. Appl. Supercond.*, **9** 2825 (1999).
2. N. McN. Alford, T. W. Button, M. J. Adams, S. Hedges, B. Nicholson, and W. A. Philips, "Low Surface Resistance in $YBa_2Cu_3O_x$ Melt-Processed Thick Films," *Nature*, **349** 680 (1991).
3. P. Selvan, E. W. Seibt, D. Kumar, R. Pinto, and P. R. Apte, "Enhanced J_c and Improved Grain-Boundary Properties of Ag-Doped $YBa_2Cu_3O_{7-\delta}$ Films," *Appl. Phys. Lett.*, **71** 137 (1997).
4. H. Kittle, M. Klauda, C. Newmann, J. Dutzi, Y. R. Li, R. Smithey, E. Brecht, R. Schneider, J. Geerk, J. Keppler, and K. Klinger, "Resonators for a 2 Pole Filter Fabricated from YBCO Coated $LaAlO_3$ Cylinders," *IEEE Trans. Appl. Supercond.*, **7** 2784 (1997).
5. J. Xu, Y. R. Li, B. W. Tao, X. Z. Liu, and H. L. Wang, "$YBa_2Cu_3O_{7-\delta}$ Thin Films with Low Surface Resistance Prepared by Self-Template Sputtering Method," *Physica*, **C331** 67 (2000).
6. X. Z. Liu, B. W. Tao, A. Luo, S. M. He, and Y. R. Li, "The Preparation of Double-Sided YBCO Thin Films by Simultaneous Sputtering from Single Target," *Thin Solid Films*, **396** 225 (2001).
7. N. Newman and W. G. Lyons, "High-Temperature Superconducting Microwave Devices: Fundamental Issues in Materials, Physics, and Engineering," *J. Supercond.*, **6** 119 (1993).
8. A. M. Hermann, J. C. Price, J. F. Scott, R. M. Yandrofski, A. Naziripour, D. Galt, H. M. Duan, M. Paranthaman, R. Tello, J. Cuchario, and R. K. Ahrenkiel, "Oxide superconductors and Ferroelectrics Materials for a New Generation of Tunable Microwave Devices," *Bull. Am. Phys. Soc.*, **38** 689 (1993).
9. A. Naziripour, A. Outzourhit, J. U. Trefny, Z.-H. Zhang, F. Barnes, J. Cleckler, and A. M. Hermann, "Fabrication of $Ba_{1-x}Sr_xTiO_3$ Tunable Capacitors with $Tl_2Ba_2Ca_1Cu_2O_x$ Electrod," *Physica*, **C233** 387 (1994).
10. A. M. Hermann, R. M. Yandrofski, J. F. Scott, A. Naziripour, D. Galt, J. C. Price, J. Cuchario, and R. K. Ahrenkiel, "Oxide Superconductors and Ferroelectrics Materials for a New Generation of Tunable Microwave Devices," *J. Supercond.*, 7 463 (1994).
11. R. A. Chakalov, Z. G. Ivanov, Y. A. Biokov, P. Larsson, E. Carlsson, S. Gevorgian, and T. Claeson, "Fabrication and Investigation of $YBa_2Cu_3O_{7-\delta}/(Ba_{0.05}Sr_{0.95})TiO_3$ Thin Film Structures for Voltage Tunable Devices," *Physica*, **C308** 279 (1998).
12. Y. Gim, T. Hudson, Y. Fan, C. Kwon, A. T. Findikoglu, B. J. Gibbons, B. H. Park, and Q. X. Jia, "Microstructure and Dielectric Properties of $Ba_{1-x}Sr_xTiO_3$ Films Grown on $LaAlO_3$ Substrates," *Appl. Phys. Lett.*, **77** 1200 (2000).
13. C. L. Canedy, H. Li, S. P. Alpay, L. Salamanca-Riba, A. L. Roytburd, and R. Ramesh, "Dielectric Properties in Heteroepitaxial $Ba_{0.6}Sr_{0.4}TiO_3$ Thin Films: Effect of Internal Stresses and Dislocation-Type Defects," *Appl. Phys. Lett.*, **77** 1695 (2000).
14. W. T. Chang, J. S. Horwitz, A. C. Carter, J. M. Pond, S. W. Kirchoefer, C. M. Gilmore, and D. B. Chrisey, "The Effect of Annealing on the Microwave Properties of $Ba_{0.5}Sr_{0.5}TiO_3$ Thin Films," *Appl. Phys. Lett.*, **74** 1033 (1999).
15. J. S. Horwitz, W. T. Chang, W. J. Kim, S. B. Qadri, J. M. Pond, S. W. Kirchoefer, and D. B. Chrisey, "The Effect of Stress on the Microwave Dielectric Properties of $(Ba_{0.5}Sr_{0.5})TiO_3$ Thin Films," *J. Electroceramics*, **4** 357 (2000).
16. Y.-A. Jeon, E.-S. Choi, T.-S. Seo, and S.-G. Yoon, "Improvements in Tunability of $(Ba_{0.5}Sr_{0.5})TiO_3$ Thin Films by Use of Metalorganic Chemical Vapor Deposited (Ba,Sr) RuO_3 Interfacial Layers," *Appl. Phys. Lett.*, **79** 1012 (2001).
17. E. J. Tarsa, E. A. Hachfield, F. T. Quinlan, J. S. Park, and M. Eddy, "Growth-Related Stress and Surface Morphology in Homoepitaxial $SrTiO_3$ Films," *Appl. Phys. Lett.*, **68** 490 (1996).
18. S. T. Lee, N. Fujimura, and T. Ito, "Epitaxial Growth of $BaTiO_3$ Thin Films and thier Internal Stresses," *Jpn. J. Appl. Phys. Part 1*, **34** 5168 (1995).
19. X. Z. Liu and Y. R. Li, "Dielectric Properties of Multilayered $SrTiO_3$ Thin Films with Graded Oxygen Vacancy Concentration," *Appl. Phys.*, **A83** 67 (2006).
20. W. T. Chang, J. S. Horwitz, A. C. Carter, J. M. Pond, S. W. Kirchoefer, C. M. Gilmore, and D. B. Chrisey, "The Effect of Annealing on the Microwave Properties of $(Ba_{0.5}Sr_{0.5})TiO_3$ Thin Films," *Appl. Phys. Lett.*, **74** 1033 (1999).
21. W. T. Chang, C. M. Gilmore, W.-J. Kim, J. M. Pond, S. W. Kirchoefer, S. B. Qadri, and D. B. Chrisey, "Influence of Strain on Microwave Dielectric Properties of (Ba,Sr)TiO_3 Thin Films," *J. Appl. Phys.*, **87** 3044 (2000).
22. C. L. Canedy, H. Li, S. P. Alpay, L. Salamanca-Riba, A. L. Roytburd, and R. Ramesh, "Dielectric Properties in Heteroepitaxial $(Ba_{0.6}Sr_{0.4})TiO_3$ Thin Films: Effect of Internal Stresses and Dislocation-Type Defects," *Appl. Phys. Lett.*, **77** 1695 (2000).
23. S. P. Alpay, I. B. Misirlioglu, V. Nagarajan, and R. Ramesh, "Can Interface Dislocations Degrade Ferroelectric Properties?," *Appl. Phys. Lett.*, **85** 2044 (2004).
24. I. B. Misirlioglu, A. L. Vasiliev, M. Aindow, S. P. Alpay, and R. Ramesh, "Threading Dislocation Generation in Epitaxial (Ba,Sr)TiO_3 Films Grown on (001) $LaAlO_3$ by Pulsed Laser Deposition," *Appl. Phys. Lett.*, **84** 1742 (2004).
25. V. Nagarajan, C. L. Jia, H. Kohlstedt, R. Waser, I. B. Misirlioglu, S. P. Alpay, and R. Ramesh, "Misfit Dislocations in Nanoscale Ferroelectric Heterostructures," *Appl. Phys. Lett.*, **86** 192910 (2005).
26. W. J. Kim, W. Chang, S. B. Qadri, J. M. Pond, S. W. Kirchoefer, D. B. Chrisey, and J. S. Horwitz, "Microwave Properties of Tetragonally Distorted $(Ba_{0.5}Sr_{0.5})TiO_3$ Thin Films," *Appl. Phys. Lett.*, **76** 1185 (2000).
27. C. M. Hanson and H. R. Beratan, "Thin Film Ferroelectrics:

Breakthrough," *Proceedings of SPIE*, **4721** 298 (2002).
28. D. F. Murphy, M. Ray, R. Wyles *et al.*, "High-Sensitivity (25-μm Pitch) Microbolometer FPAs and Application Development," *Proceedings of SPIE*, **4369** 222 (2001).
29. R. Murphy, M. Kohin, B. S. Backer *et al.*, "Recent Developments in Uncooled IR Technology," *Proceedings of SPIE*, **4028** 12 (2000).
30. M. A. Todd, P. A. Manning, P. P. Donohue *et al.*, "Thin Film Ferroelectric Materials for Microbolometer Arrays," *Proceedings of SPIE*, **4130** 128 (2000).
31. K. Sreenivas, I. Reaney, T. Maeder, N. Setter *et al.*, "Investigation of Pt/Ti Bilayer Metallization on Silicon for Ferroelectric Thin Film Integration," *J. Appl. Phys.*, **75** 232 (1994).
32. S. B. Majumder, B. Roy, R. S. Katiyar *et al.*, "Effect of Nd Doping on the Dielectric and Ferroelectric Characteristics of Sol-Gel Derived PZT Thin Films," *J. Appl. Phys.*, **90** 2975 (2001).
33. H. Han, X. Song, J. Zhong *et al.*, "Highly a-Axis-Oriented Nb-Doped $Pb(Ti_xZr_{1-x})O_3$ Thin Films Grown by Sol-Gel Technique for Uncooled Infrared Dectors," *Appl. Phys. Lett.*, **85** 5310 (2004).
34. C. G. Wu, W. L. Zhang, Y. R. Li, X. Z. Liu, J. Zhu, and B. W. Tao, "High Pyroelectric $(Ba_{0.65}Sr_{0.35})TiO_3$ Thin Films with $(Ba_{0.65}Sr_{0.35})RuO_3$ Seeding-Layer for Monolithic Ferroelectric Bolometer," *Infrared Physics & Technology*, **48** 187 (2006).
35. A. G. Chynoweth, "Spontaneous Polarization of Guanidine Aluminum Sulfate Hexahydrate at Low Temperatures," *J. Appl. Phys.*, **27** 78 (1956).